Dynamic domain motion of thermal-magnetically formed marks on CoNi/Pt multilayers

Li Zhang[a)]
Department of Applied Physics, University of Electronic Science and Technology of China, Chengdu 610054, People's Republic of China

James A. Bain and Jian-Gang Zhu
Data Storage Systems Center, Department of Electrical and Computer Engineering, Carnegie Mellon University, Pittsburgh, Pennsylvania 15213

Leon Abelmann and Takahiro Onoue
Systems and Materials for Information Storage Group, MESA+ Research Institute, University of Twente, P.O. Box 217, 7500 AE Enschede, The Netherlands

(Received 15 December 2005; accepted 19 July 2006; published online 6 September 2006)

We characterized a method of heat-assisted magnetic recording, which is potentially suitable for probe-based storage systems. The field emission current from a scanning tunneling microscope tip was used as the heating source. Various pulse voltages were applied to two types of CoNi/Pt multilayered films: one is strongly coupled with low coercivity, and the other is weakly coupled with high coercivity. Experimental results show that marks achieved in strongly coupled medium are larger than that in granular one. An external magnetic field was then applied to those marks. For weak fields (lower than the coercivity of the medium) the size of marks changes distinctly in the strongly coupled medium but not in the granular one. A model of magnetic domain dynamics is built to quantitatively explain the experimental results. It agrees with experiments. Based on this model, we will be able to figure out the proposals to achieve small marks for ultrahigh recording density.
 [DOI: 10.1063/1.2336505]

I. INTRODUCTION

The superparamagnetic effect which induces the thermal relaxation of recorded information[1] is the fundamental obstacle in increasing magnetic recording density. To achieve thermal stability of recorded information, increases in the coercivity and anisotropy of the recording medium are needed. This makes traditional recording more difficult because conventional heads cannot generate sufficient field to switch the magnetization of the bits in thermally stable media. To overcome this obstacle heat-assisted magnetic recording (HAMR) has been proposed.[2] HAMR draws on concepts from traditional magneto-optical (MO) recording for the writing process, but is not restricted to optical readback.

In addition to optical heating methods suggested by extensions of MO recording, another possible approach of HAMR is the use of field emission current from a sharp metallic tip for heating. This has the possibility of very high spatial resolution because scanning tunneling microscopes (STMs), which have similar architectures, show atomic resolution in surface observation.[3–5] Nakamura *et al.*[6] demonstrated this writing method with a STM several years ago, and observed that the mark size increased with increasing tip voltage. We have also demonstrated this process previously,[7,8] but saw very little dependence of mark size on tip voltage above a certain writing threshold. In this work, we focus on two kinds of different media to examine the influence of different magnetic parameters on the mark size. A model of magnetic domain dynamics is also executed to quantitatively explain the experimental results.

II. EXPERIMENTS

A. Recording media

The recording media in our work are two CoNi/Pt multilayered films. They are labeled as samples I and II, respectively. Each film is composed of 20 $Co_{50}Ni_{50}$(0.55 nm)/Pt(0.89 nm) bilayers, bearing a total thickness of 28 nm. Both of them were fabricated on a silicon substrate, with a 23 nm thick Pt seedlayer. The main difference of those two films is the Ar pressure during fabrication. For sample II, the Ar pressure was greatly increased, which results in the separation of grains in the film. Therefore, sample II becomes more granular with a much higher coercivity. As a result, the exchange constant A of sample II is much smaller than that of sample I. We measured their perpendicular anisotropy K_u, saturation magnetization M_S, and coercivity H_C at room temperature in a vibrating sample magnetometer (VSM). The results are listed in Table I.

TABLE I. Magnetic parameters of two samples.

	H_C				
Label	(kA/m)	(kOe)	M_S (kA/m)	K_u (J/m^3)	A (J/m)
Sample I	80	1.0	340	2.5×10^{5}	4×10^{-12}
Sample II	398	5.0	430	3.0×10^{5}	0.2×10^{-12}

[a)]Electronic mail: zhangli_cmu2005@yahoo.com.cn

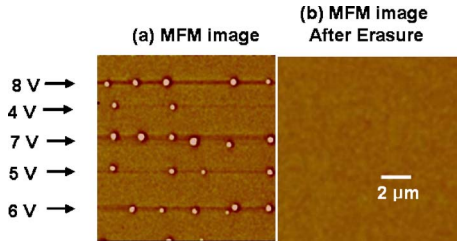

FIG. 1. (Color online) MFM images on sample I: (a) marks written by different voltages; (b) marks erased by a field of 1.6 T.

B. Writing marks

The major instrument used in experiments is a Digital Instruments Dimension 3000 scanning probe microscope (SPM). It has three operation modes: atomic force microscopy (AFM), magnetic force microscopy (MFM), and STM. Among them, AFM was applied to scan the topographic features of the film, and MFM was used to image the magnetic domain structures. STM was used for thermal writing. In this work, the STM tip is made of Ir/Pt alloy. The film was heated locally by applying pulses of 2–8 V in amplitude and 500 ns in duration, with a rise time of 100 ns to the sample. Figure 1(a) shows some marks written on sample I. In order to demonstrate that those marks are magnetic instead of magnetization damage, a strong field of 1.6 T, much greater than the coercivity of the medium, was applied to erase those marks. Figure 1(b) shows the MFM image after erasure. Because the magnetization of the sample is completely recovered, those marks are magnetic in nature, and the writing is reversible. From Fig. 1(a), we also notice that mark size varies with different voltages. The average mark size is 170–200 nm, while the minimum is 109 nm. The investigation of the average mark size as a function of the pulse voltage has been published elsewhere.[9] Similar step was done on sample II, and the average mark size is 90–120 nm, with the minimum value of 70 nm.

C. Field addition on marks

We studied the effect of external field on marks, which were written in a large matrix. The application of the external field is done after the marks are written. The direction of the external field is defined as shown in Fig. 2: (a) "negative" field is defined as the direction of field opposite to the marks, and the same as the surrounding; (b) "positive" field is defined as just opposite to the negative field defined above, meaning that it has the same direction of marks but opposite

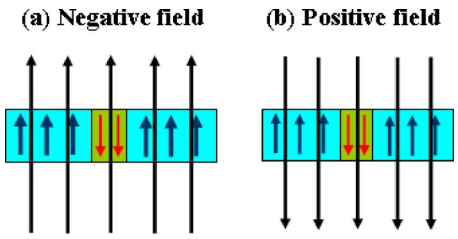

FIG. 2. (Color online) Direction of external field: (a) "negative" field, the direction of field is opposite to the marks, while the same as the surrounding; (b) "positive" field, just opposite to the negative field defined above.

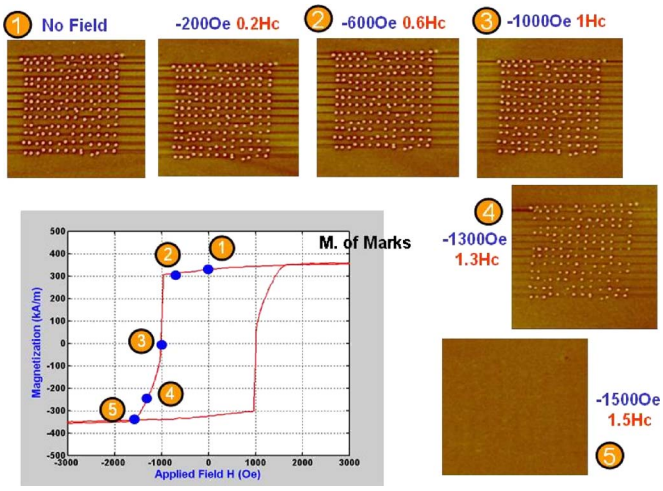

FIG. 3. (Color online) The application of negative field on the marks on sample I.

to the surrounding. In other words, negative fields oppose mark formation, while positive fields assist mark formation.

First, we worked on sample I. The effect of negative field on marks is shown in Fig. 3. Before field addition, a large matrix of marks was made on the sample. They were imaged by MFM. Then, the sample was placed in the VSM, applying a negative field of −16 kA/m (or −200 Oe, $0.20H_C$). Then the film was put back for MFM imaging. Compared to the original marks, we did not observe any change. Next step, the field is increased. Figure 3 shows the case of −48 kA/m (or −600 Oe, $0.60H_C$) a field close to the nucleation field of the film. At that point, marks begin to shrink. Then higher field is applied. An MFM image of marks after the field equivalent to the coercivity H_C (80 kA/m, or 1 kOe) was displayed. We see that the field $H=H_C$ is not enough to completely erase marks. When a field close to −104 kA/m (or, −1300 Oe, $1.30H_C$) was applied, some small marks begin to vanish. However, all of the marks are not completely erased until the field of −120 kA/m (or −1500 Oe, $1.50H_C$). Then we checked the statistics of this procedure, and plotted a curve of the percentage of marks remaining as a function of negative field, shown in Fig. 4. This behavior is similar to the hysteresis loop of *M-H* curve in Fig. 3: the percentage of marks remaining is like the dimensionless magnetization M/M_S. This step is just the amplification of the erasure process by increasing the field gradually. Thus, it is an additional demonstration of the nature of those marks: they are magnetic, instead of magnetization damage. Next, the effect of positive field on marks is shown in Fig. 5. Another large matrix of marks was made by the same tip on sample I. A small field such as +16 kA/m (or +200 Oe, $0.20H_C$) cannot move the domain wall, so the mark size does not change. With increasing field to +48 kA/m (or +600 Oe, $0.60H_C$), marks begin to expand. At the field $H=H_C$, the expansion of marks causes the domain overlap, and the magnetization is randomly orientated, with a net magnetization of zero. Then higher field is applied. Different from the negative field case above, the film does not recover to the uniform magnetization state until a field of +184 kA/m (or +2300 Oe, $2.30H_C$) was applied. A

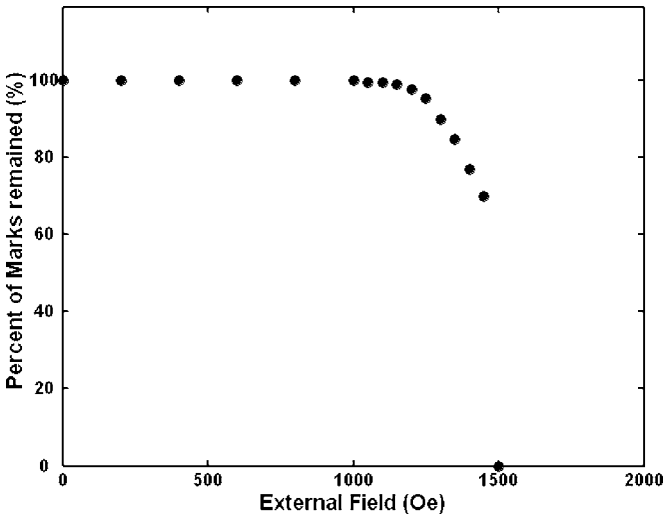

FIG. 4. Plot of the percentage of marks remaining as a function of field in the negative field application.

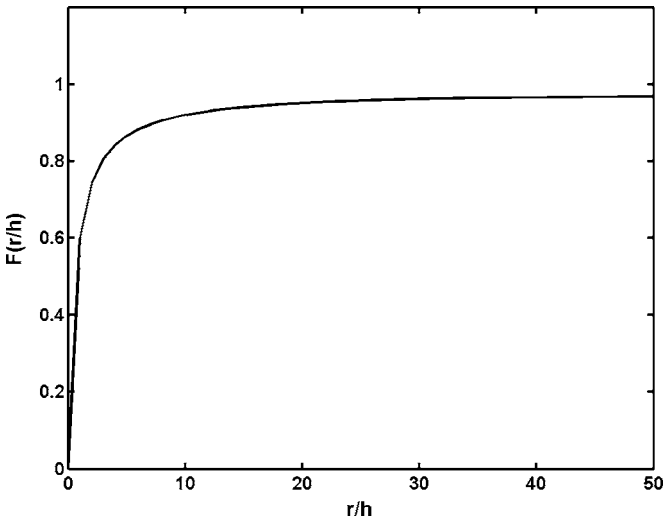

FIG. 6. Plot of magnetostatic function $f(r/h)$.

higher field is needed to completely erase those marks. The magnetization switching of the region surrounding the marks is more difficult than that of marks. The reason is that marks only take a small portion in the film, and the majority part is still the region surrounding the marks. Through this experiment, we additionally demonstrate the nature of those magnetic marks. We also found that negative field tended to shrink marks, while positive field tended to expand marks in a strongly coupled medium.

Second, we worked on Sample II. Not as many experiments were done on sample II as on sample I. For fields comparable but lower than its coercivity, we did not observe any distinct variation of mark size.

III. MODELS AND DISCUSSION

In this section, we will discuss the magnetic properties of marks on the film. Because the recording pattern is perpendicular, magnetization of marks is perpendicular to the medium plane. The isotropic heat transfer in radial direction results in circular marks in the plane.[9] We model the mark as a cylinder, with radius r and height h (or the film thickness). The magnetization is along the central axis of the cylinder. The mark is surrounded by a magnetic domain with opposite magnetization. For the strongly coupled medium such as sample I, there is a domain wall structure between the mark and its surrounding. The domain wall thickness is $\delta = \pi\sqrt{A/K_u}$,[10] 12 nm for sample I. There are several forces on the domain wall, i.e., wall surface tension $F_{\text{tension}} = 8\pi h\sqrt{AK_u}$, demagnetizing energy $F_D = \mu_0 M_S^2 \pi r h f(r/h)$, external magnetic field $F_{\text{field}} = \mu_0 M_S H 4\pi r h$, and coercive force $F_{Hc} = \mu_0 M_S H_C 4\pi r h$.[10–13] In the expression of demagnetizing energy, $f(r/h)$ is called the magnetostatic function, and expressed as[12]

$$f(t) = \frac{4t}{\pi}\int_0^1 \left(K(x) - \frac{K\{\sqrt{4x/[(1+x)^2+t^{-2}]}\}}{\sqrt{(1+x)^2+t^{-2}}} \right) x dx, \qquad (1)$$

where $K(x) = \int_0^{\pi/2} (1/\sqrt{1-x^2\sin^2\theta}) d\theta$ is the complete elliptic integral of the first kind. Function $f(r/h)$ is plotted by a numerical method in MATLAB and shown in Fig. 6. From the plot, we can see that in the case of very big mark or very thin film $r >> h$, the function approaches unity. However, it does not apply to our case, where the film thickness is 28 nm, and the radius of mark is in the range of 50–100 nm. The ratio of them is not large enough to have the function approach unity. Therefore, we need to apply the original analytical expression of the function in Eq. (1) in later analysis.

The net force per unit area on the wall is the sum of surface tension, magnetizing field, and external field. It is expressed below as (the area of domain wall is $A_{\text{wall}} = 2\pi r h$)

$$\frac{1}{2\pi r h}\frac{\Delta E}{\Delta r} = -\frac{4\sqrt{AK_u}}{r} + \frac{1}{2}\mu_0 M_S^2 f\left(\frac{r}{h}\right) \pm 2\mu_0 M_S H, \qquad (2)$$

where the negative sign means that the force is pointed inwardly to the center of mark, and positive sign means that the force is pointed outwardly from the center of mark. The sign of force from external field depends on the direction of the field. In order to determine if the domain wall will move or not, we should compare the force above with the coercive

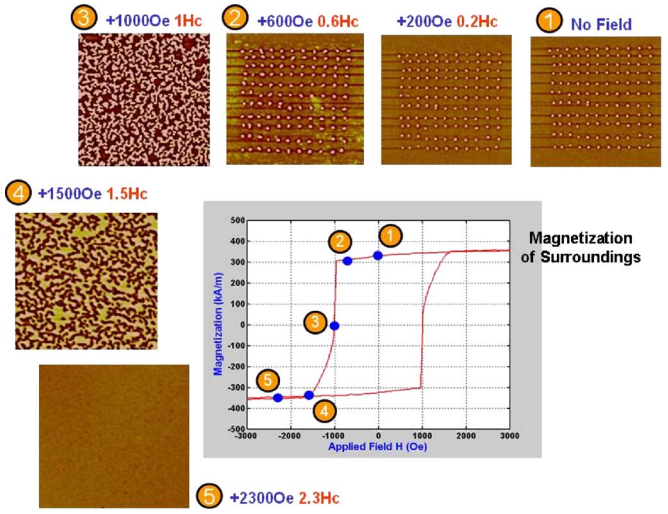

FIG. 5. (Color online) The application of positive field on the marks on sample I.

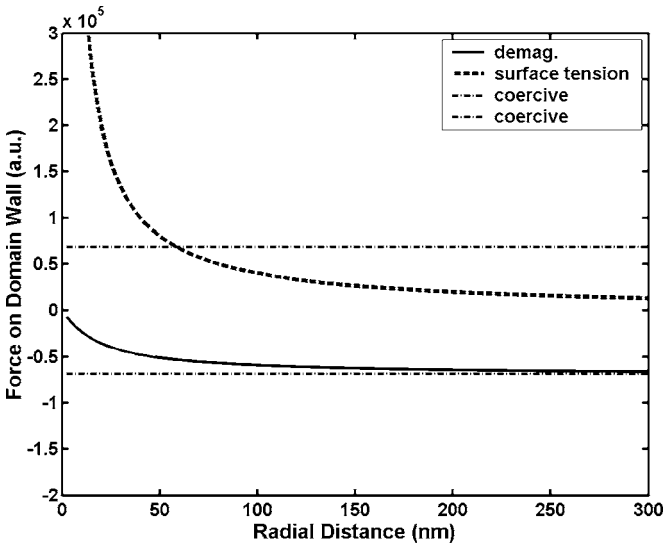

FIG. 7. Plots of several forces on domain wall as a function of radial position r: demagnetization, surface tension, and coercive force.

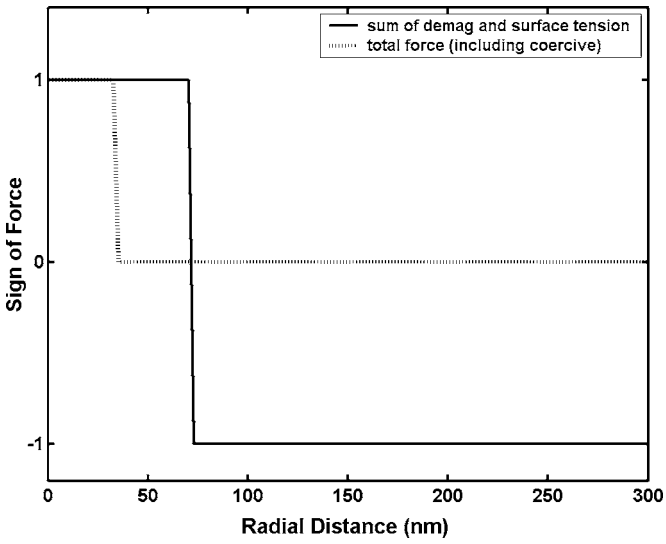

FIG. 8. Plots of the sign of force on domain wall as a function of radial position r.

force F_{H_c} (per unit area) on the domain wall.[13] The role of F_{H_c} in the perpendicular magnetic medium is similar to the static friction in mechanics. When the net force on the domain wall is smaller than the coercive force, the domain is static and does not move; once the net force on the domain wall is larger than coercive force, the domain wall starts to move. The direction of coercive force is always opposite to the net force on domain wall, i.e., the role of coercive force is to retard the motion of domain wall and try to keep equilibrium of the magnetic domain.

Now we apply the model to explain our experimental data. First, we examine sample I. Because of its abundant data, we will study this sample in details. All its magnetic parameters are stated in the last section. Figure 7 shows the plots of several forces on domain wall as a function of radial position in sample I at room temperature. We found the following properties of those forces: surface tension force increases with decreasing radius, while demagnetization has the opposite trend. For a very small mark (with radius smaller than 25 nm), surface tension will outweigh all other forces, and the domain wall will be pushed toward the center of mark, until the complete collapse of the domain. For very large marks (with radius greater than 200 nm), surface tension on the wall decays to zero, and demagnetization does not exceed the coercive force. The domain wall will not move in this case. For this film, large marks of any size will be stable. Therefore, for a strongly coupled medium, there is a lower limit of stable domain size. If the film is completely granular, the surface tension term will vanish. There will be no lower limit of stable domain size. Theoretically, a single magnetic grain can be a recording bit.

Now let us calculate the minimum stable domain size numerically. In this case, the external field is not considered because we examine the domain stability in normal data storage without applying field. According to the role of coercive force, the domain will be stable if the net force does not exceed it, i.e.,

$$\left| \frac{1}{2\pi rh} \frac{\Delta E}{\Delta r} \right| \leqslant \frac{F_{H_c}}{2\pi rh},$$

or

$$\left| -\frac{4\sqrt{AK_u}}{r} + \frac{1}{2}\mu_0 M_S^2 f\left(\frac{r}{h}\right) \right| \leqslant 2\mu_0 M_S H_C. \tag{3}$$

From Fig. 6, the magnetostatic function $f(r/h)$ does not approach unity for small radius. So we cannot get an analytical expression for the range of r from Eq. (3). Let us plot the force as a function of r in Fig. 8. For simplicity, only the signs of force (+1, −1, or 0), instead of the actual numerical value of the force, are plotted. In the figure, positive sign means that the force is pointed inwardly to the center of mark. Zero means no force on the wall. We found that $r = 72$ nm is a critical point for two forces surface tension and demagnetization. When $r < 72$ nm, surface tension exceeds demagnetization, and vise versa. However, with the function of coercive force, the domain wall does not move inwardly until the value of $r = 34$ nm. When $r > 34$ nm, the net force on the wall (the sum of surface tension and demagnetization) exceeds the coercive force, and the coercive force cannot stop the inward motion of the domain wall, until the whole domain crashes. When $r < 34$ nm, net force does not exceed the coercive force, and the domain wall does not move, so the mark is stable. Therefore, we conclude that $r_{\min} = 34$ nm (or mark size 68 nm) for sample I. That is why we did not see any mark smaller than 68 nm, which is not stable on sample I. This theory is consistent with our experimental results.

On the other hand, the upper limit of stable domain size does not exist for sample I. The reason is stated below. For very large mark, the magnetostatic function approaches unity, and the surface tension approaches zero. The net force on domain wall (without external field) will be simplified as $1/2\pi rh\Delta E/\Delta r = 1/2\mu_0 M_S^2$. The condition of domain stability will be simplified as $1/2\mu_0 M_S^2 \leqslant 2\mu_0 M_S H_C$, which is valid because $M_S \leqslant 4H_C$. That means at any location of r (as far as

it is large enough), net force is always smaller than coercive force and mark is stable. Therefore, there is no upper limit for the size of stable mark. If $M_S > 4H_C$, the upper limit for stable mark size will appear.

Now let us examine the effect of external field. In experiments, the average mark size is about 200 nm (or, radius of 100 nm) in the matrix of marks. Calculated from Eq. (2), we found that when negative field is greater than $0.8H_C$ and positive field greater than $0.9H_C$, the net force on the domain wall will exceed the coercive force and the domain wall begins to move. Although it is higher than experimental value $0.6H_C$, the agreement is good.

Next, we briefly work on sample II. By repeating the above calculation of the minimum stable domain size, we found that the minimum stable domain size is less than 5 nm. This value is very close to the grain size of the film. Theoretically, a single magnetic grain can be a recording bit in sample II. In experiments, we did not see any marks smaller than this theoretical value, or it is beyond the ability of our current instrumentation and recording media. On the other hand, the calculated domain wall thickness from $\delta = \pi\sqrt{\frac{A}{K_u}}$ is about 2 nm, which is comparable or even smaller than the size of a single magnetic grain. In this case, the domain wall structure does not exist. Regarding the effect of field addition on marks, the first term of Eq. (2) can be neglected. And we found that the external field lower than the coercivity of the film cannot change the mark size. It agrees with experimental results.

In summary, this model works well for two CoNi/Pt multilayered films with different magnetic properties. From this model, we found that the coercivity and the exchange constant of the film determine the minimum stable domain size. By increasing the coercivity and decreasing the exchange constant of the film, we will achieve smaller and smaller stable marks. In this way, we will be able to increase the recording density in this medium.

IV. CONCLUSION

We have demonstrated a thermomagnetic writing process using a STM on perpendicular CoNi/Pt multilayered media. Results show that smaller marks can be achieved on a higher coercivity and weakly coupled medium. For field addition, positive field increases mark size, and negative field reduces mark size when they reach some threshold values. A model of magnetic domain wall motion was executed quantitatively to examine our data and it agrees with experiments well. Based on this model, we found a direction to increase the recording density in data storage systems: increasing the coercivity and reducing the exchange constant of the recording medium.

ACKNOWLEDGMENTS

This work is part of a project on MEMS-based magnetic mass storage systems[14] at the Center for Highly Integrated Information Processing and Storage Systems (CHIPSs) in Carnegie Mellon University, USA. This work was funded in part by NASA through Grant No. NAG8-1799.

[1] P. L. Lu and S. H. Charap, IEEE Trans. Magn. **31**, 2767 (1995).
[2] J. J. M. Ruigrok, R. Coehoorn, S. R. Cumpson, and H. W. Kesteren, J. Appl. Phys. **87**, 5398 (2000).
[3] G. Binnig, H. Rohrer, Ch. Gerber, and W. Weibel, Phys. Rev. Lett. **49**, 57 (1982).
[4] G. Binnig, H. Rohrer, Ch. Gerber, and W. Weibel, Appl. Phys. Lett. **40**, 178 (1982).
[5] G. Binnig, H. Rohrer, Ch. Gerber, and W. Weibel, Phys. Rev. Lett. **50**, 120 (1983).
[6] J. Nakamura, M. Miyamoto, S. Hosaka, and H. Koyanagi, J. Appl. Phys. **77**, 779 (1995).
[7] L. Zhang, J. A. Bain, and J.-G. Zhu, IEEE Trans. Magn. **38**, 1895 (2002).
[8] L. Zhang, J. A. Bain, J.-G. Zhu, L. Abelmann, and T. Onoue, IEEE Trans. Magn. **40**, 2549 (2004).
[9] L. Zhang, J. A. Bain, J.-G. Zhu, L. Abelmann, and T. Onoue, J. Magn. Magn. Mater. 305, 16 (2006).
[10] A. A. Thiele, A. H. Bobeck, E. D. Torre, and U. F. Gianola, Bell Syst. Tech. J. **50**, 711 (1971).
[11] A. A. Thiele, Bell Syst. Tech. J. **50**, 725 (1971).
[12] M. Mansuripur and G. A. N. Connell, J. Appl. Phys. **55**, 3049 (1984).
[13] H. D. Shieh and M. H. Kryder, J. Appl. Phys. **61**, 1108 (1987).
[14] L. R. Carley *et al.*, J. Appl. Phys. **87**, 6680 (2000).